Proceedings of the 28th IEEE
EMBS Annual International Conference
New York City, USA, Aug 30-Sept 3, 2006

Comparison of Different Wavelet Subband Features in the Classification of ECG Beats Using Probabilistic Neural Network

Ying-Hsiang Chen and Sung-Nien Yu
yhchen@samlab.ee.ccu.edu.tw, yusn@ee.ccu.edu.tw
Department of Electrical Engineering, National Chung Cheng University, Taiwan

***Abstract*—In this paper, an electrocardiogram (ECG) beat classification system based on wavelet transformation and probabilistic neural network (PNN) is proposed to discriminate six ECG beat types. The effects of two wavelet decomposition structures, the two-stage two-band and the two-stage full binary decomposition structures, in the recognition of ECG beat types are studied. The ECG beat signals are first decomposed into components in different subbands using discrete wavelet transformation. Three statistical features of each decomposed subband signals as well as the AC power and instantaneous RR interval of the original signal are exploited to characterize the ECG signals. A PNN then follows to classify the feature vectors. The result shows that features extracted from the decomposed signals based on the two-stage two-band structure outperform the two-stage full binary structure. A promising accuracy of 99.65%, with equally well recognition rates of over 99% throughout all type of ECG beats, has been achieved using the optimal feature set. Only 11 features are needed to attain this performance. The results demonstrate the effectiveness and efficiency of the proposed method for the computer-aided diagnosis of heart diseases based on ECG signals.**

I. Introduction

THE recognition and classification of the electrocardiogram (ECG) beat is an important subject for diagnosing different cardiac diseases. In recent years, many algorithms have been developed for the detection and classification of the ECG beat [1]-[4]. Although these methods have shown impressive results in some classification tasks, they usually failed to demonstrate equally well discrimination throughout all types of ECG beats. Wavelet transformation (WT) opens another category of methods that represent the signal in different translations and scales. Furthermore, the discrete wavelet transformation (DWT) decomposes a signal into signals of different coarseness. Features extracted from the wavelet coefficients were capable of effectively representing the characteristics of the original signal.

However, because a signal can be decomposed in different ways and the number of features grows quickly with the number of stages, we designated to study the effects of different subband features in the classification of ECG beats. The objective is to find an efficient and effective combination of subband features for ECG beat recognition.

In this study, we consider two wavelet decomposition structures, in which different combinations of subband features are extracted and their effects on ECG classification are investigated. Besides of the features extracted from the decomposed signals, the instantaneous RR interval is considered as another feature and its effect is justified.

We use a probabilistic neural network (PNN) to test the performance of different feature sets. The PNN classifier is a kind of artificial neural network (ANN) classifier, which is noted for its simplicity and generality. Comparing with the most popular ANN, the multilayer perceptron (MLP), PNN considerably reduces the intensive computation in the MLP [5]. Therefore, we choose PNN as the classifier for the comparison of different wavelet subband feature combinations in the recognition of six ECG beat types.

II. Method

A. Discrete wavelet transformation (DWT)

Discrete wavelet transformation has been widely used in signal processing tasks. The major advantage of the DWT is that it provides great time and frequency localization. Moreover, the multi-scale feature of the DWT allows the decomposition of an ECG signal into different scales. Among various wavelet bases, the Haar wavelet is the shortest and simplest basis that provides satisfactory localization of signal characteristics in time domain [6]. Therefore, the Haar wavelet was chosen as the mother wavelet in this study.

There exist several wavelet decomposition structures. The two most popular wavelet decomposition structures are illustrated in Fig. 1. The wavelet decomposition structures in Fig. 1 show two stages of decomposition. In each stage, the input signal is decomposed into two subband signals, which is called a DWT of order two. Theoretically, each decomposed signal is obtained by convoluting the input signal with a specific filter and down-sampling the filtered signal. A high-pass filter, $g(n)$, and a low-pass filter, $h(n)$, are employed in the decomposition process. These filters are derived from the Haar mother wavelet and can be mathematically expressed as

$$g(n)=\left\{\frac{1}{\sqrt{2}},-\frac{1}{\sqrt{2}}\right\}, \quad (1)$$

$$h(n)=\left\{\frac{1}{\sqrt{2}},\frac{1}{\sqrt{2}}\right\}. \quad (2)$$

Apparently, these filters based on Haar wavelet are capable of performing an orthonormal multiresolution analysis of a signal. The symbol $\downarrow 2$ represents down-sampling the filtered signal by two.

Fig. 1(a) is the two-stage two-band decomposition

structure, in which only the low-pass filtered signal in the first stage is further decomposed in the second stage. On the contrary, Fig. 1(b) shows the two-stage full binary decomposition tree structures, in which both of the decomposed signals in the first stage are further decomposed in the second stage. In the consequence, the input signal is decomposed into three subband signals in the LL, LH, and H bands, as illustrated in Fig. 1(a), while is decomposed into four subband signals in the LL, LH, HL, and HH bands in Fig. 1(b). Theoretically, an input signal of $N=2^k$ can be decomposed in at most k stages. In this study, we decompose the original signals with DWT for two stages.

B. Feature extraction

Several features obtained from the decomposed signal in different subband are used to characterize these signals.

1) Signal Variance:

The signal variance in a subband represents the average AC power in that band. With a discrete-time signal x of N samples, the signal variance is defined as

$$\sigma_x^2 = \frac{1}{N}\sum_{n=1}^{N}\left[x(n)-\bar{x}\right]^2 \tag{3}$$

where $\bar{x}$ is the sample mean of the signal. The variances of the original and decomposed signal are the first feature set in our method, which are denoted in Table 1 as σ_x for the original signal and P for the subband signals.

2) Variance of the Autocorrelation Function of a Signal:

The autocorrelation function can be used as a measure of similarity or coherence between a signal *x(n)* and its shifted version. If *x(n)* is of length *N*, its autocorrelation function is expressed as

$$R_{xx}(l) = \sum_{n=i}^{N-|k|-1} x(n)x(n-l) \tag{4}$$

where l is the time shift index, $i=l$, $k=0$ for $l \geqq 0$, and $i=0$, $k=l$ for $l<0$. The variance of the autocorrelation, σ_R, represents the averaged AC power of the autocorrelation function, which measures the coherence of the decomposed signal in each subband [7]. Thus, we use it as the second feature set.

3) Relative Amplitude:

The relative amplitude of the decomposed signal *x(n)* for each subband is defined as

$$Q = \min\left(x(n)\right)/\max\left(x(n)\right) \tag{5}$$

which represents the morphological characteristics of the signal and is regarded as the third feature set used in our proposed method.

4) RR Interval:

Certain ECG arrhythmia, such as APB and PVC, are related with premature heart beats that provide shorter RR intervals than other types of ECG signals. Therefore, we exploit the instantaneous RR interval as another feature, which is defined as the time duration between the two adjacent R peaks.

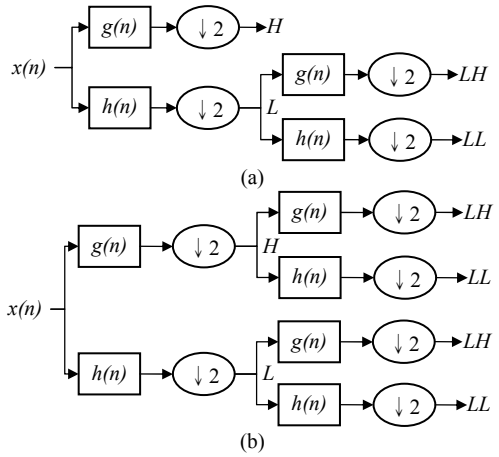

Fig. 1. Two wavelet decomposition structures: (a) the two-stage two-band decomposition structure, and (b) the two-stage full binary structure for discrete wavelet transformation, where *h(n)* is the low-pass filter and *g(n)* is the high-pass filter.

C. Normalization of feature vectors

Because the quantities of the features may be quite different, a normalization process is necessary to standardize all the features to the same level. The formula of the normalization is defined as follows:

$$x_{ij}' = \text{tansig}\left(\frac{x_{ij}-\bar{x}_j}{\sigma_{x_j}}\right) \tag{6}$$

where x_{ij} is the j-th component of the i-th feature vector, $\bar{x}_j$ and σ_{xj} are the mean and standard deviation, respectively, of the j-th component of the feature vectors, and tansig(·) is a hyperbolic tangent sigmoid transfer function. The expression in the brackets makes the j-th component to be normal distributed with zero-mean and unity standard deviation. The hyperbolic tangent sigmoid function maps a wide-ranged signal to that with limited range [-1, +1]. In our experiment, the mean and the standard deviation of each component in the feature vectors are calculated from the training dataset and are used throughout the experiments.

D. Classification using the probabilistic neural network

Probabilistic neural network (PNN) is a special type of radial basis-function networks [5]. The structure of the PNN classifier consists of three layers, an input layer, a hidden layer, and an output layer. The input layer is merely a distribution layer. No computation is performed in this layer. The hidden layer is also called the pattern layer. Neurons in the hidden layer utilize multi-dimensional kernels to estimate the probability density function for classification. One of the most popular kernels is Gaussian function since it guarantees the convergence of the neural network. The output layer is a competition layer. The number of neurons in the competition layer is the same as that of the desired classes, i.e. six neurons

in the competition layer in our experiments.

E. Experimental procedure

The QRS complex of the ECG signal associates with the electrical ventricular activation of the heart and is one of the most important ECG features. We extracted the QRS complexes from the ECG data files for the study. Based on the R-peak position labeled in the annotation file provided by the MIT/BIH database [8], 64-point QRS segments centered at R-peaks were extracted from the record.

After the DC value of each QRS segment was removed, the DC-free QRS segment was decomposed with the two wavelet decomposition structures introduced in Section II.A. For each decomposed signal in individual subband, the three features described in Section II.B were calculated and normalized to characterize the signal.

To investigate the influence of different wavelet decomposition structures in ECG beat classification, we consider different feature sets obtained in different decomposition structures. The feature sets selected for this study are summarized in Table 1, in which the feature sets F1 to F5 are obtained from the full binary decomposition structure while feature sets F6 and F7 are obtained from the two-stage two-band decomposition structure.

F1 consists of features extracted from all of the four subbands in the full binary decomposition structure. To evaluate the importance of different subband signals, we eliminate features from one subband and formulate feature sets F2 to F5 for different combinations of subband features. Similarly, feature sets F6 and F7 consist of features extracted from the decomposed signals in the two-stage two-band decomposition structure. The only difference between F6 and F7 is that the RR interval is included in F6 but not in F7. Please note that, besides of features extracted from the wavelet decomposition, the variance of the original ECG beat signal is included in F1 to F7 and the instantaneous RR interval is included in F1 to F6. With this arrangement, the influence of the RR interval on ECG beat classification can be revealed by comparing the result using F7 with that using other feature sets.

Table 1: Different feature set used to characterize QRS complexes. σ_x is the variance of the original signal, σ_R is the variance of the autocorrelation function, P is the power of the decomposed signal, Q is the relative morphological characteristic, RRI is the successive RR interval, and N is the number of features for the corresponding feature set.

		F1	F2	F3	F4	F5	F6	F7
x[n]	σ_x	✓	✓	✓	✓	✓	✓	✓
L	σ_R							
	P							
	Q							
H	σ_R						✓	✓
	P						✓	✓
	Q						✓	✓
LL	σ_R	✓	✓	✓	✓		✓	✓
	P	✓	✓	✓	✓		✓	✓
	Q	✓	✓	✓	✓		✓	✓
LH	σ_R	✓	✓	✓		✓	✓	✓
	P	✓	✓	✓		✓	✓	✓
	Q	✓	✓	✓		✓	✓	✓
HL	σ_R	✓	✓		✓	✓		
	P	✓	✓		✓	✓		
	Q	✓	✓		✓	✓		
HH	σ_R	✓		✓	✓	✓		
	P	✓		✓	✓	✓		
	Q	✓		✓	✓	✓		
RRI		✓	✓	✓	✓	✓	✓	
N		14	11	11	11	11	11	10

III. Results and Discussion

The MIT-BIH arrhythmia database [8] contains 48 records from 47 subjects. To eliminate possible bias due to lacking of sufficient pathological beats in certain records, we exclude the records that contain very small number of ECG beats and select the 23 representative ECG records for analysis and recognition. These records include six ECG beat types which are the normal beat (N), the left bundle branch block beat (LBBB), the right bundle branch block beat (RBBB), the atrial premature beat (APB), the premature ventricular contraction(PVC), and the paced beat (PB). This process results in totally 23200 QRS complexes extracted from the 23 records ready for analysis. Half of these segments are used as the training data set, and the other half are used as the test set. For the purpose of conformity, signals recorded with ML II are exploited in the experiments.

Three statistics indices are employed to evaluate the performance of our proposed method, which are defined, separately, as follows

$$specificity = \frac{\#\text{ of correct classified normal beats}}{\#\text{ of total normal beats}} \quad (7)$$

$$sensitivity = \frac{\#\text{ of correct classified abnormal beats}}{\#\text{ of total corresponding abnormal beats}} \quad (8)$$

$$accuracy = \frac{\#\text{ of correct classified beats}}{\#\text{ of total beats}} \quad (9)$$

The classification results, represented as specificity (sep.), sensitivity (sen.), and overall classification accuracy (acc.), are summarized in Table 2. The results are impressive: wavelet subband features in both different decomposition structures demonstrate imposing classification accuracies. Amongst them, F6 achieves the highest average accuracy of 99.65% and F5 has the lowest average accuracy of 98.65%. However, all of the feature sets under study demonstrate their high capabilities for discriminating different ECG beat types.

Recall that F1~F5 are feature sets extracted based on the two-stage full binary decomposition structure. In this category of subband feature sets, F5 shows the lowest accuracy. Since F5 contains all the subband features except those extracted from the LL subband, we infer that the

features in the LL subband must play an important role in characterizing ECG beat signals. When examining the results of these feature sets more closely, we discover that F1~F4 can distinguish most individual ECG beat type very concisely. However, lower sensitivities are observed in the recognition of PVC and APB. Therefore, we conclude that the feature set extracted from the full binary wavelet decomposition structure may have good performance in the average sense, but still can not achieve equally well discrimination power among all types of ECG beats under study.

The feature sets F6~F7 are extracted from the two-stage two-band decomposition structure. Among the seven feature sets, F6 demonstrates the highest average accuracy. As shown in Table 2, all of the statistical performance indices for the F6 are greater than 99%. The result demonstrates that F6 can provide equally well discrimination power throughout all ECG beat types. Additionally, the importance of RR interval in discriminating premature beat types is revealed by comparing the results of using F6 and F7 in classification. As mentioned in Section II.E, F7 consists of the same features as F6 except the RR interval. The result shows that, without the information of RR interval, the sensitivities of premature beat types are lowered. This experiment demonstrates the importance of RR interval in the recognition of certain types of ECG beats, such as PVC and APB.

It is also interesting to compare our method with other ECG beat recognition systems presented in the literatures [1]-[4]. The optimal result of using F6 is used to represent our method for comparison. Table 3 compares the accuracy of these systems. The result shows that the proposed method provides a higher classification accuracy than the other systems. However, it is noted that, although the same MIT-BIH database was utilized to testify the performance of these systems, different numbers of beat types belonging to different patient records were selected to conduct the experiments. Therefore, it is difficult to compare the result fairly. Only the averaged accuracy and the overall performance of the systems are justified.

IV. Conclusions

In this study, we proposed an ECG classification scheme based on wavelet transform and PNN classifier. Two wavelet decomposition structures and the associated subband features were used and their performance in ECG beat classification was compared. Subband features extracted from the two-stage two-band wavelet decomposition structure together with the RR interval are proven to be the optimal feature set for this task. The optimal feature set achieves a promising accuracy of 99.65% and equally outstanding discrimination power of over 99% throughout all types of ECG beats under study. The number of features need to attain this high accuracy is only 11, which is substantially lower than that in the other methods. From the results, we conclude that different pathological changes in ECG beats can be faithfully represents by the three categories of features extracted from the decomposed waveforms. The instantaneous RR interval plays an important role to further furnish the capability of the system, especially in the discrimination of high risk heart diseases such as PVC and APB. This study proves that the proposed method is an excellent model for the computer-aided diagnosis of heart diseases based on ECG signals.

Table 2: Classification results with different feature sets.

	Spe.	Sen. (%)					Acc.
	(%)	LBBB	RBBB	PVC	APB	PB	(%)
F1	99.97	99.50	99.33	98.61	99.06	99.92	99.54
F2	99.89	99.38	99.38	98.87	99.65	99.92	99.57
F3	99.94	99.38	99.50	98.17	99.06	99.92	99.50
F4	99.97	99.38	99.54	98.26	98.94	99.92	99.52
F5	99.86	97.96	97.79	97.65	97.41	99.83	98.65
F6	99.97	99.33	99.54	99.04	99.76	99.92	99.65
F7	99.86	99.04	99.42	97.65	98.82	99.92	99.32

Table 3: Comparison of different ECG beat classification methods.

Method	Number of beat types	Accuracy
Proposed	6	99.65%
FHyb-HOSA [1]	7	96.06%
MME [2]	5	97.78%
Neuro-Fuzzy [3]	4	98.00%
MLP-Fourier [4]	3	98%

Acknowledgment

This study was supported in part by the grant NSC94-2213-E-194-049 from the National Science Council, Taiwan, R.O.C.

References

[1] Stanislaw Osowski and Tran Hoai Linh, "ECG beat recognition using fuzzy hybrid neural network," *IEEE Trans. Biomed. Eng., Vol. 48, No. 11,* Nov. 2001.

[2] İnan Güler and Elif Derya Übeyli, "A modified mixture of experts network structure for ECG beats classification with diverse features," *Engineering Applications of Artificial Intelligence, Vol. 18,* Oct. 2005, pp. 845-856.

[3] Mehmet Engin, "ECG beat classification using neuro-fuzzy network," *Pattern Recognition Letters, Vol. 25,* Nov. 2004, pp. 1715-1722.

[4] K. Minami, H. Nakajima, and T. Toyoshima, "Real-time discrimination of ventricular tachyarrhythmia with Fourier-transform neural network," *IEEE Trans. Biomed. Eng., Vol. 46, No. 2,* Feb. 1999, pp. 179-185.

[5] Wasserman P. D., *Advanced Methods in Neural Computing*. VNR Press, 1992, Ch. 3.

[6] J. F. Scholl, J. R. Agre, L. P. Clare, and M. C. Gill, "A low power impulse signal classifier using the Haar wavelet transform," in *Proc. SPIE, Sensors,* 1999, pp 136-145.

[7] S. K. Goumas, M. E. Zervakis, and G. S. Stavrakakis, "Classification of washing machines vibration signals using discrete wavelet analysis for feature extraction," *IEEE Trans. Instrumentation and Measurement, Vol. 51, No. 3,* Jun. 2002, pp. 497-508.

[8] Physiobank Archieve Index, MIT-BIH Arrhythmia Database: http://www.physionet.org/physiobank/database (Access time: 10th December 2003).